Machine Copy for Proofreading, Vol. x, y–z, 2013

NUMERICAL METHOD OF COMPUTING THE IMPEDANCE OF A TWIN HIGH CURRENT BUSDUCT OF RECTANGULAR HOLLOW CONDUCTORS

Joanna Kolanska-Pluska[1], Pawel Jablonski[2], and Zygmunt Piatek[3, *]

[1]Opole University of Technology, 76, Proszkowska Street, Opole 45-758, Poland

[2]Czestochowa University of Technology, 17, Armii Krajowej Av., Czestochowa 42-200, Poland

[3]Czestochowa University of Technology, 60A, Brzeznicka Street, Czestochowa 42-200, Poland

Abstract—In this paper, a new numerical method of calculating the total impedance of a twin high current busduct consisting of rectangular hollow busbar is proposed. The method is based on the integral equation method and partial inductance theory. Results for impedance of this twin high current busduct have been obtained, and the skin and proximity effects have also been taken into consideration. The validation of the proposed method is carried out through Finite Element Method (FEM) and laboratory measurements, and a reasonable level of accuracy is demonstrated.

1. INTRODUCTION

In the process of induction heating of metals the inductor is often powered by a single phase transmission line in the form of rectangular hollow conductor. This allows simultaneous cooling the track with running water flowing inside the phase conductors [1–4]. One example of the power systems with internal coil in the induction hardened pipe loads is shown in Fig. 1.

Accurate calculation of impedance of the twin high current busduct and inductor is especially important during parameter selection of supply source. There are many approximate methods

Received 28 August 2013.

* Corresponding author: Zygmunt Piatek (zygmunt.piatek@interia.pl).

Figure 1. Induction heater setup: 1 — high current busduct (bandaged), 2 — inner inductor, 3 — workpiece (heated cylindrical element).

of determining the self and mutual inductance of rectangular busbar trunking system, e.g., described in [5–16]. Their resistance with the skin effect can be determined using graphs given in [17] in the case of hollow square copper tubes, only. The geometric mean distance method makes the self inductance possible to determine for any hollow rectangular conductor but in the case of DC only [18]. There is no analytical formula for the mutual inductance between two hollow rectangular busbars. So this study paper describes a new numerical method of computing the total impedance (resistance, self and mutual inductances) of a twin high current busduct of rectangular hollow conductors and the skin and proximity effects are also taken into consideration.

2. ALGORITHM FOR DETERMINING THE TOTAL IMPEDANCE

Let us consider a system of two rectilinear profiled lines of rectangular cross-section and possibly different lengths l_1 and l_2, made of non-ferromagnetic material of magnetic permeability μ_0 and electrical conductivity σ (Fig. 2).

Suppose that between the two ends of the twin feeder there are forced time-harmonic voltages of complex values $\underline{U}_1$ and $\underline{U}_2$ and angular frequency ω. If $\underline{I}_1$ is the current in the system, then

$$\underline{Z} = \frac{\underline{U}_1 - \underline{U}_2}{\underline{I}_1}. \tag{1}$$

The impedance can be also found via electromagnetic field theory. The electric field at point $\mathbf{X}$ has the potential part $-\nabla \underline{V}(\mathbf{X})$ and the

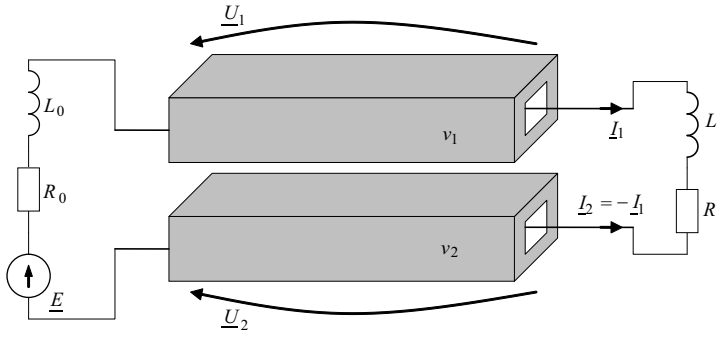

Figure 2. Computational model of rectangular hollow current busduct.

induced part $-j\omega\underline{\mathbf{A}}(\mathbf{X})$, and the resultant electric field equals

$$\underline{\mathbf{E}}(\mathbf{X}) = -\nabla\underline{V}(\mathbf{X}) - j\omega\underline{\mathbf{A}}(\mathbf{X}) \tag{2}$$

with

$$\underline{\mathbf{A}}(X) = \frac{\mu_0}{4\pi}\sum_{n=1}^{2}\int_{\nu_n}\frac{\underline{\mathbf{J}}(Y)dx_2dy_2dz_2}{\sqrt{(x_1-x_2)^2+(y_1-y_2)^2+(z_1-z_2)^2}} \tag{3}$$

where $X = X(x_1,\, y_1,\, z_1)$ is the point of observation, $Y = Y(x_2,\, y_2,\, z_2)$ is the source point, and ν_n is the volume of n-th line, $n = 1,\, 2$.

Having regard to the Ohm's law

$$\underline{\mathbf{J}} = \sigma\underline{\mathbf{E}} \tag{4}$$

and Equations (2) and (3), common integral equation [6, 7] is obtained:

$$\frac{1}{\sigma}\underline{\mathbf{J}}(x_1,y_1,z_1)+j\omega\frac{\mu_0}{4\pi}\sum_{n=1}^{2}\int_{\nu_n}\frac{\underline{\mathbf{J}}(x_2,y_2,z_2)dx_2dy_2dz_2}{\sqrt{(x_1-x_2)^2+(y_1-y_2)^2+(z_1-z_2)^2}}$$
$$= -\nabla\underline{V}(x_1,y_1,z_1) \tag{5}$$

In order to obtain the numerical solution of Equation (5), the volume of integration of individual lines shall be divided into elements in the form of rectangular subbars. Due to specific shape of the busbars, each of them can be considered as consisting of four bars making its walls (see Fig. 3).

Each bar is then divided into subbars, the cross section area of which is:

$$\Delta S^{(p)} = \Delta x^{(p)}\Delta y^{(p)} \tag{6}$$

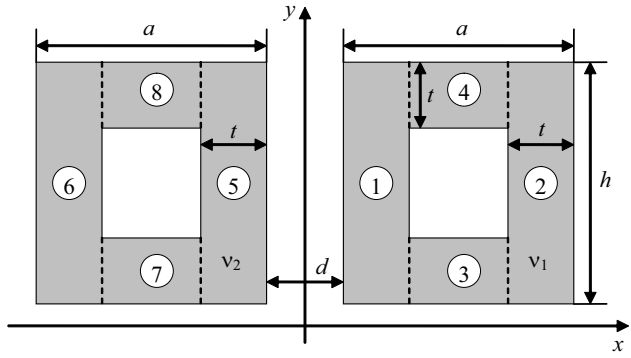

Figure 3. Busduct division into bars (cross-section).

with

$$\Delta x^{(p)} = \frac{X_2^{(p)} - X_1^{(p)}}{N_x^{(p)}}, \quad \Delta y^{(p)} = \frac{Y_2^{(p)} - Y_1^{(p)}}{N_y^{(p)}} \tag{7}$$

where $(X_1^{(p)},\ Y_1^{(p)})$ and $(X_2^{(p)},\ Y_2^{(p)})$ are coordinates of the left bottom and right top corners of the cross-section of p-th subbar, $p = 1, 2, \ldots, 8$, and $N_x^{(p)}$ and $N_y^{(p)}$ are the numbers of divisions of the cross-section along directions x and y (see Fig. 4).

The domain of k-th subbar of p-th bar is denoted as $\nu_k^{(p)}$. Let $N^{(p)} = N_x^{(p)} N_y^{(p)}$ be the total number of subbars within each bar. The

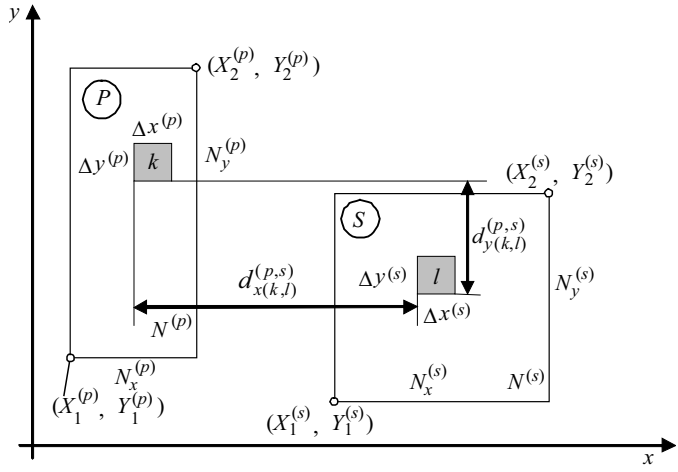

Figure 4. Bars division into subbars (cross-section).

total current in each subbar, $\underline{I}_k^{(p)}$, $p = 1, 2, \ldots, 8$, $k = 1, 2, \ldots, N^{(p)}$, is assumed to have constant density as below

$$\underline{\mathbf{J}}(x_1, y_1, z_1)|_{(x_1,y_1,z_1)\in\nu_k^{(p)}} = \frac{\underline{I}_k^{(p)}}{\Delta S^{(p)}}\mathbf{a}_{z_1} \tag{8}$$

where $\mathbf{a}_{z_1}$ is a unit vector in the direction of z_1 axis.

In Equation (5), approximation (8) is substituted and the integral over regions ν_1 and ν_2 is expressed as the sum of integrals over subbars $\nu_k^{(p)}$. Then the equation is dotted with $\mathbf{a}_{z_1}$ and integrated over subbar $\nu_l^{(s)}$. As a consequence, the resulting equation can be written as follows:

$$R_l^{(s)}\underline{I}_l^{(s)} + j\omega\sum_{p=1}^{8}\sum_{k=1}^{N^{(p)}} M_{l,k}^{(s,p)}\underline{I}_k^{(p)} = \underline{U}_l^{(s)} \tag{9}$$

where

$$R_l^{(s)} = \frac{l^{(s)}}{\sigma\Delta S^{(s)}} \tag{10}$$

is the DC resistance of subbar $\nu_l^{(s)}$ and

$$M_{l,k}^{(s,p)} = \frac{\mu_0}{4\pi}\frac{1}{\Delta S^{(s)}\Delta S^{(p)}}\int\limits_{\nu_l^{(s)}}\int\limits_{\nu_k^{(p)}}\frac{dx_1dy_1dz_1dx_2dy_2dz_2}{\sqrt{(x_1-x_2)^2+(y_1-y_2)^2+(z_1-z_2)^2}} \tag{11}$$

is the DC mutual inductance between subbars $\nu_l^{(s)}$ and $\nu_k^{(p)}$.

Inductances $M_{l,k}^{(s,p)}$ are expressed by sextuple integral, but they can be evaluated analytically [6, 7]. This is of particular importance if $\nu_l^{(s)} = \nu_k^{(p)}$ (when the volume integral is calculated twice over the same subbar), because then the integral becomes improper, and its numerical computation would therefore be difficult.

By adopting the notation as shown in Fig. 5, sextuple integral (11) can be considered as a function of nine variables

$$M\left(\Delta x^{(p)}, \Delta x^{(s)}, \Delta y^{(p)}, \Delta y^{(p)}, l^{(p)}, l^{(s)}, d_{x(k,l)}^{(p,s)}, d_{y(k,l)}^{(p,s)}, d_{z(k,l)}^{(p,s)}\right)$$

$$= \frac{\mu_0}{4\pi}\frac{1}{\Delta x^{(p)}\Delta y^{(p)}\Delta x^{(s)}\Delta y^{(s)}} \times \int\limits_{x_1=0}^{\Delta x^{(p)}}\int\limits_{y_1=0}^{\Delta y^{(p)}}\int\limits_{z_1=0}^{l^{(p)}}\int\limits_{x_2=d_{x(k,l)}^{(p,s)}}^{d_{x(k,l)}^{(p,s)}+\Delta x^{(s)}}\int\limits_{y_2=d_{y(k,l)}^{(p,s)}}^{d_{y(k,l)}^{(p,s)}+\Delta y^{(s)}}$$

$$\int\limits_{z_2=d_{z(k,l)}^{(p,s)}}^{d_{z(k,l)}^{(p,s)}+l^{(s)}}\frac{dx_1dy_1dz_1dx_2dy_2dz_2}{\sqrt{(x_1-x_2)^2+(y_1-y_2)^2+(z_1-z_2)^2}}, \tag{12}$$

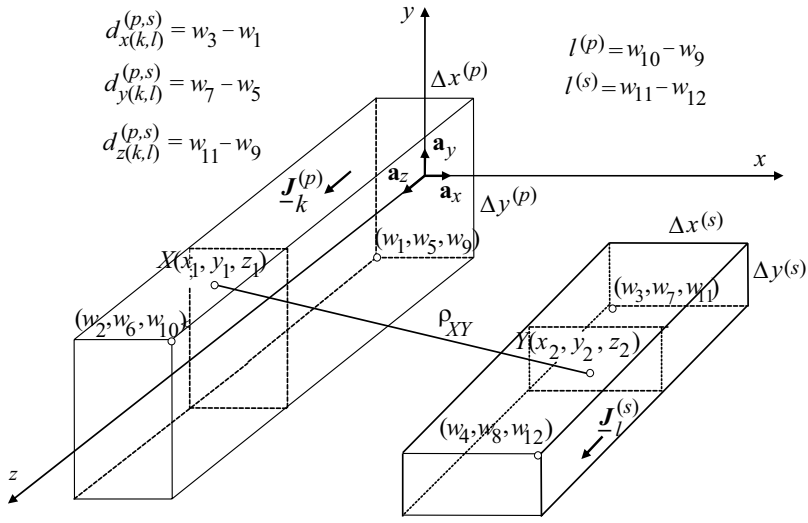

Figure 5. Parameters defining the position of two subbars; $w_1, w_2, \ldots, w_{12}$ determine coordinates of opposite corner points of subbars (p, k) and (s, l)

where $l^{(p)}$, $l^{(s)}$ are the lengths of subbars, $\Delta x^{(p)}$, $\Delta x^{(s)}$, $\Delta y^{(p)}$, $\Delta x^{(s)}$ are the transverse dimensions of the subbars, and $d^{(p,s)}_{x(k,l)}$, $d^{(p,s)}_{y(k,l)}$, $d^{(p,s)}_{z(k,l)}$ are the offsets between the subbars along the axes x, y, z. These symbols are defined in Figs. 4 and 5.

Function (12) of nine variables is an analytical function. In the considered busduct, $d^{(p,s)}_{z(k,l)} = 0$, $l^{(p)} = l^{(s)} = l$. Furthermore, if we assume $\Delta x^{(p)} = \Delta x^{(s)} = \Delta x$, $\Delta y^{(p)} = \Delta y^{(s)} = \Delta y$, and denote shortly d_x for $d^{(p,s)}_{x(k,l)}$ and d_y for $d^{(p,s)}_{y(k,l)}$, then the following function of five variables $M(\Delta x, \Delta y, l, d_x, d_y)$ will be obtained:

$$M(\Delta x, \Delta y, l, d_x, d_y) = \frac{\mu_0}{4\pi} \frac{1}{(\Delta x \Delta y)^2} \int_{x_1=0}^{\Delta x} \int_{y_1=0}^{\Delta y} \int_{z_1=0}^{l} \int_{x_2=d_x}^{d_x+\Delta x} \int_{y_2=d_y}^{d_y+\Delta y} \int_{z_2=0}^{l} \frac{dx_1 dy_1 dz_1 dx_2 dy_2 dz_2}{\sqrt{(x_1-x_2)^2 + (y_1-y_2)^2 + (z_1-z_2)^2}} \quad (13)$$

However, these simplifications are not crucial, because the accurate solution was obtained as a result of complex integrations of formula (13), without any simplifying assumptions, in accordance to

formula (20) described in [6]:

$$M\left(\Delta x^{(p)}, \Delta x^{(s)}, \Delta y^{(p)}, \Delta y^{(p)}, l^{(p)}, l^{(s)}, d^{(p,s)}_{x(k,l)}, d^{(p,s)}_{y(k,l)}, d^{(p,s)}_{z(k,l)}\right)$$
$$= \frac{\mu_0}{4\pi} \frac{1}{\Delta x^{(p)} \Delta y^{(p)} \Delta x^{(s)} \Delta y^{(s)}} \sum_{i=1}^{4} \sum_{j=1}^{4} \sum_{k=1}^{4} (-1)^{i+j+k+1} F(\alpha_i, \beta_j, \gamma_k) \quad (14)$$

where

$$\begin{aligned}
\alpha_1 &= d^{(p,s)}_{x(k,l)} - \Delta x^{(p)}, \quad & \alpha_2 &= d^{(p,s)}_{x(k,l)} + \Delta x^{(s)} - \Delta x^{(p)}, \\
\alpha_3 &= d^{(p,s)}_{x(k,l)} + \Delta x^{(s)}, \quad & \alpha_4 &= d^{(p,s)}_{x(k,l)}, \\
\beta_1 &= d^{(p,s)}_{y(k,l)} - \Delta y^{(p)}, \quad & \beta_2 &= d^{(p,s)}_{y(k,l)} + \Delta y^{(s)} - \Delta y^{(p)}, \\
\beta_3 &= d^{(p,s)}_{y(k,l)} + \Delta y^{(s)}, \quad & \beta_4 &= d^{(p,s)}_{y(k,l)}, \\
\gamma_1 &= d^{(p,s)}_{z(k,l)} - l^{(p)}, \quad & \gamma_2 &= d^{(p,s)}_{z(k,l)} + l^{(s)} - l^{(p)}, \\
\gamma_3 &= d^{(p,s)}_{z(k,l)} + l^{(s)}, \quad & \gamma_4 &= d^{(p,s)}_{z(k,l)}
\end{aligned} \quad (15)$$

and [6]

$$F(x,y,z) = \frac{1}{72}[F_1(x,y,z) + F_1(y,z,x) + F_1(z,x,y)] \quad (16)$$

where

$$F_1(x,y,z) = \frac{6}{5}x^2\left(x^2-3y^2\right)\sqrt{x^2+y^2+z^2} - 12x^3yz\tan^{-1}\frac{yz}{x\sqrt{x^2+y^2+z^2}}$$
$$-3x\left(y^4 - 6y^2z^2 + z^4\right)\ln\left(x + \sqrt{x^2+y^2+z^2}\right) \quad (17)$$

The self inductance is obtained in the singular case, when the subbars overlap themselves:

$$L(\Delta x, \Delta y, l) = \lim_{d^{(p,s)}_{x(k,l)} \to 0} \lim_{d^{(p,s)}_{y(k,l)} \to 0} \lim_{d^{(p,s)}_{z(k,l)} \to 0} M(\Delta x, \Delta x, \Delta y, \Delta y, l, l, d^{(p,s)}_{x(k,l)}, d^{(p,s)}_{y(k,l)}, d^{(p,s)}_{z(k,l)}), \quad (18)$$

which after evaluating the limits yields [6]:

$$L(\Delta x, \Delta y, l)$$
$$= \frac{\mu_0}{120\pi(\Delta x \Delta y)^2}[F_2(\Delta x, \Delta y, l) + F_2(\Delta y, l, \Delta x) + F_2(l, \Delta x, \Delta y)] \quad (19)$$

where

$$\begin{aligned}
&F_2(x,y,z)\\
&=4x^5+4\left(x^4-3x^2y^2+y^4\right)\sqrt{x^2+y^2}+4x^2\left(x^2-3y^2\right)\sqrt{x^2+y^2+z^2}\\
&-40x^3yz\tan^{-1}\frac{yz}{x\sqrt{x^2+y^2+z^2}}+30x^2y^2z\ln\frac{\sqrt{x^2+y^2+z^2}+z}{\sqrt{x^2+y^2+z^2}-z}\\
&-5x\left[y^4\ln\frac{\left(\sqrt{x^2+y^2+z^2}+x\right)\left(\sqrt{x^2+y^2}-x\right)}{\left(\sqrt{x^2+y^2+z^2}-x\right)\left(\sqrt{x^2+y^2}+x\right)}\right.\\
&\left.+z^4\ln\frac{\left(\sqrt{x^2+y^2+z^2}+x\right)\left(\sqrt{x^2+z^2}-x\right)}{\left(\sqrt{x^2+y^2+z^2}-x\right)\left(\sqrt{x^2+z^2}+x\right)}\right]
\end{aligned}\tag{20}$$

Since function (11) is known now, the system of integral Equation (5) can be discretized according to Equation (9). Equations (10) and (11) yield the following matrix elements of the system of Equation (9):

$$\underline{Z}_{l,k}^{(s,p)}=R_l^{(s)}\delta_{s,p}\delta_{l,k}+j\omega M_{l,k}^{(s,p)}\tag{21}$$

where $\delta_{i,j}$ is Kronecker delta. The system of Equation (9) can now be rewritten in the form of

$$\sum_{p=1}^{8}\sum_{k=1}^{N^{(p)}}\underline{Z}_{l,k}^{(s,p)}\underline{I}_k^{(p)}=\underline{U}_l^{(s)}\tag{22}$$

Equation (22) is solved with respect to currents $\underline{I}_k^{(p)}$. Therefore, the reverse matrix (admittance matrix) shall be computed:

$$\underline{\mathbf{Y}}=\left[\underline{Y}_{l,k}^{(s,p)}\right]=\left[\underline{Z}_{l,k}^{(s,p)}\right]^{-1}\tag{23}$$

and thus, from Equation (22) it follows that:

$$\underline{I}_k^{(p)}=\sum_{s=1}^{8}\sum_{l=1}^{N^{(s)}}\underline{Y}_{l,k}^{(s,p)}\underline{U}_l^{(s)}\tag{24}$$

Total current in m-th busbar can be expressed by the formula

$$\underline{I}_m=\sum_{p=4(m-1)+1}^{4m}\sum_{k=1}^{N^{(p)}}\underline{I}_k^{(p)}\tag{25}$$

or by using Equation (24) in (25):

$$\underline{I}_m = \sum_{p=4(m-1)+1}^{4m} \sum_{k=1}^{N^{(p)}} \sum_{s=1}^{8} \sum_{l=1}^{N^{(s)}} \underline{Y}_{l,k}^{(s,p)} \underline{U}_l^{(s)} \tag{26}$$

The voltage $\underline{U}_l^{(s)}$ for subbars belonging to the same busbar are as follows:

$$\underline{U}_l^{(s)} = \begin{cases} \underline{U}_1 & \text{for } 1 \le s \le 4 \\ \underline{U}_2 & \text{for } 5 \le s \le 8 \end{cases} \tag{27}$$

Thus, Equation (26) can now be written as:

$$\underline{I}_m = \sum_{p=4(m-1)+1}^{4m} \sum_{k=1}^{N^{(p)}} \sum_{n=1}^{2} \sum_{s=4(n-1)+1}^{4n} \sum_{l=1}^{N^{(s)}} \underline{Y}_{l,k}^{(s,p)} \underline{U}_n \tag{28}$$

After changing the order of summation it becomes:

$$\underline{I}_m = \sum_{n=1}^{2} \left[\sum_{p=4(m-1)+1}^{4m} \sum_{k=1}^{N^{(p)}} \sum_{s=4(n-1)+1}^{4n} \sum_{l=1}^{N^{(s)}} \underline{Y}_{l,k}^{(s,p)} \right] \underline{U}_n \tag{29}$$

If we define

$$\underline{Y}_{m,n} = \sum_{p=4(m-1)+1}^{4m} \sum_{k=1}^{N^{(p)}} \sum_{s=4(n-1)+1}^{4n} \sum_{l=1}^{N^{(s)}} \underline{Y}_{l,k}^{(s,p)} \tag{30}$$

then Equation (29) will take the form as follows:

$$\underline{I}_m = \sum_{n=1}^{2} \underline{Y}_{m,n} \underline{U}_n = \underline{Y}_{m,1} \underline{U}_1 + \underline{Y}_{m,2} \underline{U}_2 \tag{31}$$

or after solving it with respect to $\underline{U}_n$:

$$\underline{U}_n = \sum_{m=1}^{2} \underline{Z}_{m,n} \underline{I}_m = \underline{Z}_{1,n} \underline{I}_1 + \underline{Z}_{2,n} \underline{I}_2 \tag{32}$$

where

$$\left[\underline{Z}_{m,n}\right] = \left[\underline{Y}_{m,n}\right]^{-1} \tag{33}$$

According to Equation (1), the total impedance of the busduct equals then

$$\begin{aligned} \underline{Z} &= \frac{\left[\underline{Z}_{1,1}\underline{I}_1 + \underline{Z}_{1,2}(-\underline{I}_1)\right] - \left[\underline{Z}_{2,1}\underline{I}_1 + \underline{Z}_{2,2}(-\underline{I}_1)\right]}{\underline{I}_1} \\ &= \underline{Z}_{1,1} + \underline{Z}_{2,2} - \underline{Z}_{1,2} - \underline{Z}_{2,1} \end{aligned} \tag{34}$$

3. EXPERIMENTAL AND NUMERICAL VALIDATIONS

The computational model was verified using the busduct shown in Fig. 6. Table 1 shows the values of geometric and supply parameters used during numerical simulations and experimental measurements. The busduct was made of copper ($\sigma = 56\,\mathrm{MS/m}$).

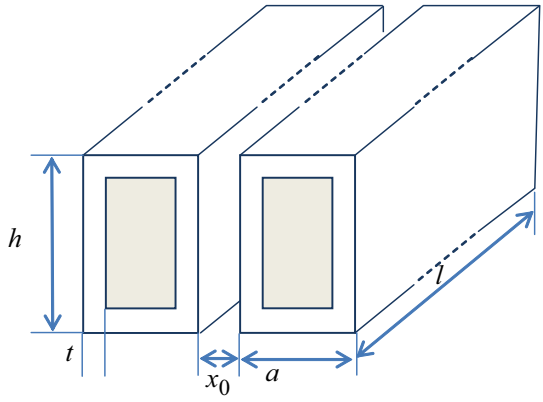

Figure 6. The busduct under consideration.

Table 1. Parameter values of the busduct under consideration.

l [mm]	a [mm]	h [mm]	t [mm]	x_0 [mm]
2100	10	13,5	2	3

The busduct was also modeled in Finite Element Method Magnetics (FEMM) software (Fig. 7), which solves Helmholtz equation for vector magnetic potential using 2D finite elements [19].

In order to verify the computed total impedance of the busduct, also measurements were performed. The busduct supplied the inductor of induction heater used in hardening the inner surfaces of cylindrical charges (Fig. 8). During operation the system was cooled with water. The current and voltage were measured with use of a digital recorder both on the input terminals of the system and the inductor terminals. The total impedance was computed by Ohm's law for the first harmonic of voltage and current. The current was taken via Rogowski coil CWT 30 B.

The results of computations and measurements of the total impedance of the high-current busduct under consideration are presented in Table 2.

As seen from Table 1, values of impedance evaluated with different methods and measured agree on acceptable level of accuracy.

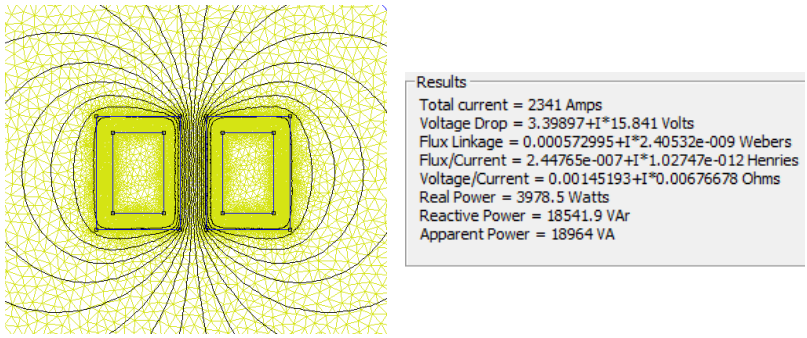

Figure 7. Cross-section of the conductors in FEMM.

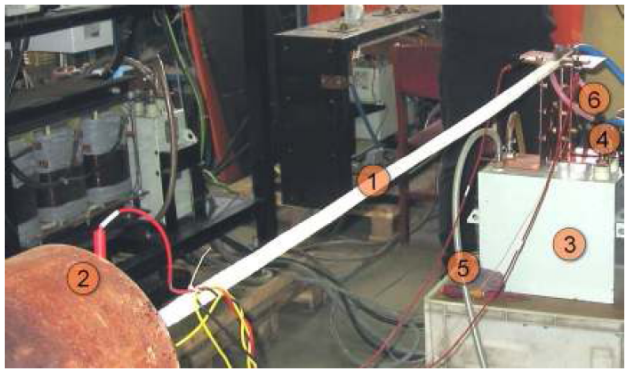

Figure 8. Measurement setup for high-current busduct impedance: 1 — bandaged busduct, 2 — heated element (workpiece), 3 — power inverter, 4 — supply, 5 — cooling pipes, 6 — Rogowski coil.

Table 2. The total impedance of the considered high-current busduct.

f [Hz]	Proposed method	FEMM	Measurements
0	$R=0.916\,[\mathrm{m\Omega}]$	$R=0.9156\,[\mathrm{m\Omega}]$	–
50	$\underline{Z}=0.89+j0.26\,[\mathrm{m\Omega}]$	$\underline{Z}=0.96+j0.20\,[\mathrm{m\Omega}]$	$\underline{Z}=0.92+j0.23\,[\mathrm{m\Omega}]$
1000	$\underline{Z}=1.53+j3.96\,[\mathrm{m\Omega}]$	$\underline{Z}=1.63+j3.83\,[\mathrm{m\Omega}]$	$\underline{Z}=1.44+j5.77\,[\mathrm{m\Omega}]$
4400	$\underline{Z}=2.97+j15.23\,[\mathrm{m\Omega}]$	$\underline{Z}=2.76+j12.69\,[\mathrm{m\Omega}]$	$\underline{Z}=2.81+j16.19\,[\mathrm{m\Omega}]$
10000	$\underline{Z}=4.38+j30.18\,[\mathrm{m\Omega}]$	$\underline{Z}=4.55+j28.47\,[\mathrm{m\Omega}]$	$\underline{Z}=4.34+j28.03\,[\mathrm{m\Omega}]$

4. CONCLUSIONS

This paper describes the method of computing the total impedance of a twin high current busduct of rectangular hollow conductors. The busduct can be used to supply the inductor for induction heater. Total impedance value of the busduct was computed, taking into account the effect of load-back, which has particular meaning during the stage of designing and selecting parameters for the supply source. Computations of impedance were performed for several values of frequency using formula (34). The computational and experimental values of the total impedance stay in agreement on a reasonable level, which is a confirmation of validity of the computational model presented in the paper.

REFERENCES

1. Barglik, J., I. Doležel, P. Karban, I. Kwiecień, and B. Ulrych, "Comparison of two ways of induction hardening of long steel tubes," *Proc. of the XIII Int. Sym. on Theoretical Electrical Engineering, ISTET'05*, 11–14, Lvov, 2005.
2. Davies, E. J., *Conduction and Induction Heating*, Peter Peregrinus Ltd., London, 1990.
3. Rudnev, V., et al., *Handbook of Induction Heating*, Marcel Dekker, New York, 2003.
4. Kolańska-Płuska, J., J. Barglik, B. Baron, and Z. Piatek, "Inductance of tubular high current busduct of rectangular finite length," *Electrical Review*, Vol. 87, 138–141, 2011.
5. Paul, C. R., *Inductance: Loop and Partial*, J Wiley & Sons, New Jersey, 2010.
6. Piątek, Z. and B. Baron, "Exact closed form formula for self inductance of conductor of rectangular cross section," *Progress In Electromagnetics Research M*, Vol. 26, 225–236, 2012.
7. Piątek, Z., et al., "Exact closed form formula for mutual inductance of conductors of rectangular cross section," *Przegląd Elektrotechniczny (Electrical Review)*, R. 89, No. 3a, 61–64, 2013.
8. Piątek, Z., B. Baron, P. Jablonski, D. Kusiak, and T. Szczegielniak, "Numerical method of computing impedances in shielded and unshielded three-phase rectangular busbar systems," *Progress In Electromagnetics Research B*, Vol. 51, 135–156, 2013.
9. Fazljoo, S. A. and M. R. Besmi, " A new method for calculation of impedance in various frequencies," *1st Power Electronic & Drive*

Systems & Technologies Conference (PEDSTC), 36–40, Feb. 17–18, 2010.

10. Sarajčev, P. and R. Goič, "Power loss computation in high-current generator bus ducts of rectangular cross-section," *Electric Power Components and Systems*, No. 39, 1469–1485, 2010.
11. Broydé, F., E. Clavelier, and L. Broydé, "A direct current per-unit-length inductance matrix computation using modified partial inductance," *Proc. of the CEM 2012 Int. Symp. on Electromagnetic Compatibility*, Rouen, Apr. 25–27, 2012.
12. Hoer, C. and C. Love, "Exact inductance equations for rectangular conductors with application to more complicated geometries," *J. Res. NBS*, Vol. 69C, No. 2, 127–137, 1965.
13. Canova, A. and L. Giaccone, "Numerical and analytical modeling of busbar systems," *IEEE Trans. on Power Delivery*, Vol. 24, No. 3, 1568–1577, Jul. 2009.
14. Matsuki, M. and A. Matsushima, "Improved numerical method for computing internal impedance of a rectangular conductor and discussions of its high frequency behavior," *Progress In Electromagnetics Research M*, Vol. 23, 139–152, 2012.
15. Matsuki, M. and A. Matsushima, "Efficient impedance computation for multiconductor transmission lines of rectangular cross section," *Progress In Electromagnetics Research B*, Vol. 43, 373–391, 2012.
16. Battauscio, O., M. Chiampi, and D. Chiarabaglio, "Experimental validation of a numerical model of busbar systems," *IEE Proceedings — Generation, Transmission and Distribution*, 65–72, 1995.
17. Copper Development Association, *Copper for Busbars*, 2001, Available Online at: http://www.cda.org.uk/Megab2/elecapps/pub22/index.htm.
18. Kalantarov, P. L. and L. A. Tseitlin, *Inductance Calculations*, Energiya, Saint Petersburg, 1970 (in Russian).
19. Meeker, D. C., *Finite Element Method Magnetics*, Version 4.2, Apr. 11, 2012, Mathematica Build, http://www.femm.info.